Research Article

Journal of Environmental Nanotechnology

Green Synthesis of Tungsten Trioxide Nanoparticles Using *Selenicereus undatus* Peel Extract and their Characterization

S. Auxilia Ruby[1*], J. Felicita Florence[1] and H. Asia Thabassoom[2]

[1]PG and Research Department of Chemistry, Holy Cross College (A), Affiliated to Bharathidasan University, Tiruchirappalli, TN, India
[2]PG and Research Department of Chemistry, Jamal Mohamed College (A), Affiliated to Bharathidasan University, Tiruchirappalli, TN, India
Received: 28.12.2024 Accepted: 15.02.2025 Published: 30.03.2025
*auxiliaruby@gmail.com

ABSTRACT

This study presents an eco-friendly and innovative approach for the synthesis of tungsten trioxide nanoparticles (WO_3 NPs) using *Selenicereus undatus* (white fleshed dragon fruit) peel extract, aligning with the principles of green chemistry. The synthesis process was meticulously optimized by varying key parameters, such as precursor concentration, pH, temperature, and reaction time. The optimal conditions were determined to be a 2:1 ratio of *Selenicereus undatus* peel extract to 0.5 M sodium tungstate, a pH of 5, an incubation temperature of 100°C for a duration of 2.5 hours. Characterization of the synthesized WO_3 NPs revealed critical structural and functional properties. The XRD analysis confirmed a monoclinic crystalline structure with an average crystallite size of 41.57 nm. FTIR spectroscopy validated the presence of W–O–W and W=O bonds, while UV-DRS analysis showed indirect band gap energy of 2.23 eV. The SEM and EDS investigations elucidated the surface morphology and elemental composition of WO_3 NPs. Furthermore, DLS and zeta potential measurements demonstrated uniform size distribution and good colloidal stability. This research highlights the efficacy of *Selenicereus undatus* peel extract as a sustainable and green stabilizing agent in the synthesis of tungsten trioxide nanoparticles, paving the way for their promising applications across diverse fields of nanoscience and nanotechnology.

Keywords: Green synthesis; Tungsten trioxide; *Selenicereus undatus;* Zeta potential.

1. INTRODUCTION

The increasing demand for sustainable and eco-friendly materials has driven significant interest in green synthesis techniques for nanoparticle production. Unlike conventional chemical synthesis methods, which often involve hazardous chemicals and generate toxic by-products, green synthesis employs environmentally benign resources, such as plant extracts, microorganisms, or agricultural bio-waste. This approach not only reduces environmental impact but also aligns with the principles of green chemistry, offering a cost-effective and sustainable alternative for nanomaterial development (Mahdi *et al.* 2021).

Agricultural bio-waste, which is often discarded, presents a rich source of bioactive compounds that can be utilized for green synthesis. *Selenicereus undatus* peel, a by-product of the fruit industry, is one such promising material. Despite its disposal in large quantities, the peel contains a wealth of bioactive constituents, including phenolic compounds, flavonoids, and antioxidants, making it an excellent candidate for reducing and stabilizing agents in nanoparticle synthesis (Joice *et al.* 2023). These compounds not only facilitate the reduction of metal ions but also impart functional properties to the synthesized nanoparticles, enhancing their biological and chemical performance. The valorization of dragon fruit peel in this context not only adds value to the agricultural waste but also contributes to a circular economy by minimizing waste and promoting resource efficiency (Irudayaraj *et al.* 2024).

WO_3 NPs have gained considerable attention due to their exceptional properties, including high thermal stability, excellent photocatalytic activity, and remarkable radiation shielding capabilities (Ghazal *et al.* 2022). These characteristics make WO_3 NPs highly suitable for applications in catalysis, environmental remediation, energy storage, and shielding against harmful radiation. Incorporating dragon fruit peel as a green additive for the synthesis of WO_3 NPs offers a dual advantage of exploiting bioactive compounds in the peel for eco-friendly synthesis and enhancing the functional properties of the nanoparticles (Aminuzzaman *et al.* 2019).

This study explores the green synthesis of tungsten trioxide nanoparticles using dragon fruit peel as a sustainable and bioactive additive. By harnessing the natural reducing and stabilizing agents in dragon fruit peel, the research aims to develop an efficient,

environmentally friendly method for producing WO_3 NPs with superior properties. Furthermore, the study underscores the potential of agricultural bio-waste in advancing sustainable nanotechnology, contributing to both environmental protection and technological innovation.

2. MATERIALS AND METHODS

Selenicereus undatus fruit were procured from an organic agro farm in Dharmapuri district, Tamil Nadu, India, during the peak harvesting season (June–August). The chemicals required for synthesis, including sodium tungstate dihydrate ($Na_2WO_4 \cdot 2H_2O$, extra pure AR 99%), sodium hydroxide pellets (NaOH, extra pure AR 98%), and 0.5 N hydrochloric acid (HCl), were sourced from Sisco Research Laboratories Pvt. Ltd. (SRL), Maharashtra, India. Deionized (DI) water and absolute ethyl alcohol (99.9%), used for extraction and synthesis, were obtained from Changshu Hongsheng fine chemical Co. Ltd.

Fig. 1: Photograph showing (a) peels of *Selenicereus undatus*, (b) chopped peels of *Selenicereus undatus*, (c) coarse powder, (d) extract under maceration and (e) methanolic extract of *Selenicereus undatus*

2.1 Preparation of *Selenicereus undatus* Extract

The freshly procured pesticide-free *Selenicereus undatus* (SU) fruit were thoroughly washed with running water followed by deionized (DI) water to remove any dirt or impurities. The peels were manually separated from the pulp, and non-essential parts such as the flower end pit, fins, bracts, and areoles were carefully removed. The percentage recovery of peel from the pulp was calculated to estimate the average biowaste generated.

$$\% \text{ Recovery of peel} = \frac{\text{Weight of SU peels (g)}}{\text{Total weight of SU (g)}} \times 100 \quad \ldots (1)$$

The peels were finely chopped, oven-dried at 70°C, and ground into a coarse powder using a laboratory pulverizer. Among various extraction methods, the widely used maceration technique was employed. The coarse peel biomass was soaked in methanol for 96 hours in a maceration chamber to facilitate the release of bioactive compounds into the extract. The solubilization of these compounds was visually indicated by a noticeable color change in the solvent and the fading color of the peel. The methanol extract was then separated from the peels and stored at 4°C for further analysis. Fig. 1 illustrates the step-by-step stages of *Selenicereus undatus* peel extraction using maceration method.

2.2 Factors Influencing WO_3 NPs Synthesis

Optimization involves developing a methodology to enhance a material's properties and functionality. In nanotechnology, key factors influencing the successful formation of nanoparticles include size, shape, yield, stability, and synthesis method. Several parameters, such as precursor concentration, the ratio of additive to precursor, pH, temperature, and reaction time, were systematically optimized. The ideal conditions were optimized from the maximum yield and absorbance of Ultraviolet-Visible (UV-Vis) spectrophotometer. The additive-to-precursor ratio (SU extract: $Na_2WO_4 \cdot 2H_2O$) was tested in varying ratios (1:1, 1:2, 1:3, 2:1, 3:1, 2:3, and 3:2). Similarly, the concentration of $Na_2WO_4 \cdot 2H_2O$ was varied across different concentrations (1 M, 0.5 M, 0.1 M, 0.05 M, 0.01 M, 0.005 M, and 0.001 M). The pH conditions were adjusted from 1 to 13, stabilized with 0.1 N HCl and 0.1 N NaOH. Reaction time was tested between 30 minutes to 3.5 hours to determine the optimal duration, while incubation temperature was varied from 40°C to 100°C for high nanoparticle yield (Rizvi *et al.* 2022). All trials were labeled, and absorbance was measured using the UV-Vis spectrophotometer in the range 200–800 nm. The synthesis process was initially optimized by varying the concentration of the precursor. For each concentration, the yield of the product and the corresponding absorbance peak were analyzed to determine the optimal conditions. The precursor concentration that resulted in the highest yield and a desirable absorbance peak were fixed. This optimized concentration was subsequently used as a baseline for further experiments involving the variation of other

synthesis parameters. Similarly, the concentration of the additive precursor, pH, incubation temperature and time were optimized and fixed following the same procedure for subsequent experiments.

Fig. 2: Photograph illustrating different stages of reaction between the additive and precursor under acidic medium

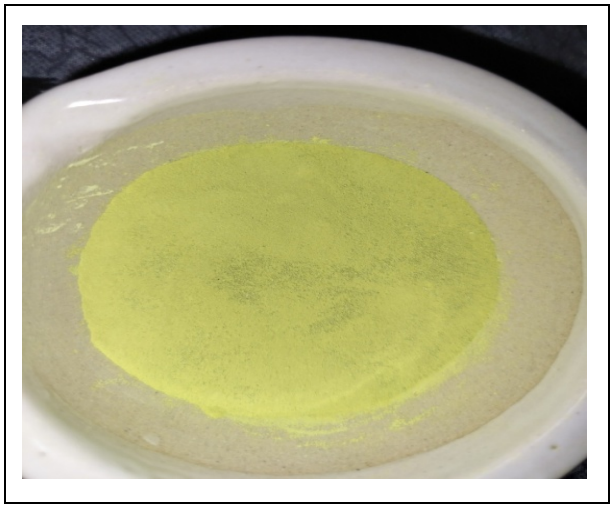

Fig. 3: Photograph displaying the pale yellowish WO_3 NPs

2.3 Green Synthesis of *Selenicereus undatus* Peel Mediated WO_3 NPs

The synthesis process was developed based on optimized conditions determined through various trials with different parameters. In this procedure, 100 mL of *Selenicereus undatus* peel extract was mixed with 50 mL of a 0.5 M $Na_2WO_4 \cdot 2H_2O$ solution. The reaction was conducted under constant stirring using a magnetic stirrer for 2.5 hours. The pH of the solution was maintained at 5, and the incubation temperature was kept at 100°C. At the beginning of the reaction, the solution exhibited a noticeable color change, transitioning from pale yellow to dark green and finally to navy blue, accompanied by the formation of precipitates when the pH was decreased. With continued incubation, the solution yielded a pale yellow precipitate, as depicted in Fig. 2. The resulting nanoparticles were separated from the reaction mixture through centrifugation at 12,000 rpm for 15 minutes. The solid product was thoroughly washed multiple times with methanol and deionized water to eliminate impurities, followed by additional centrifugation steps. The purified nanoparticles were then dried in a vacuum dryer at 90°C for 36 hours. Finally, the dried nanoparticles were subjected to calcination in a muffle furnace at 600°C for 3 hours to ensure complete crystallization and purity.

2.4 Physicochemical Characterization of WO_3 NPs

Green synthesized WO_3 NPs were characterized using various analytical techniques to determine their physical, optical, and structural properties. FTIR spectrophotometry (Shimadzu IRAFFINITY -1) was employed (4000 cm^{-1} to 400 cm^{-1}), to determine the functional groups present in the synthesized nanoparticles in a form a pellets of 10 mm diameter utilizing the 1% mixture of anhydrous KBr optical transparent salt and WO_3 NPs using a manual hydraulic press machine (Specac M-33). Furthermore, the optical properties of WO_3 NPs were analyzed using a UV-Visible spectrophotometer (Perkin Elmer Lambda 35) in the range 200–800 nm. P-XRD analysis (Bruker D8 Advance, Panalytical X Pert3) was conducted using a Cu-Kα radiation source with a 2θ range of 5° to 90°. XRD provided insights into the crystal structure, nature of crystallinity, lattice parameters, and orientation based on the diffraction patterns (Pechyen *et al.* 2024). Additionally, the crystalline size was calculated using Debye-Scherrer equation, where the most intense peak of 2θ was employed for the determination. The morphology and surface topology of the green-synthesized WO_3 NPs were examined using SEM (Carl Zeiss EVO 18), equipped with BSD detectors for enhanced topology information. The high resolution of SEM facilitated close focus and magnification of the densely packed specimens, offering a detailed visualization of their shape and size. Elemental analysis was carried out using EDAX, which confirmed the presence of desired elements and ensured minimal impurities in the material. The average particle size and stability of the colloidal suspension of the nanoparticles were evaluated using dynamic light scattering (DLS) and

zeta potential measurements (Zetasizer Advance – Malvern Panalytical).

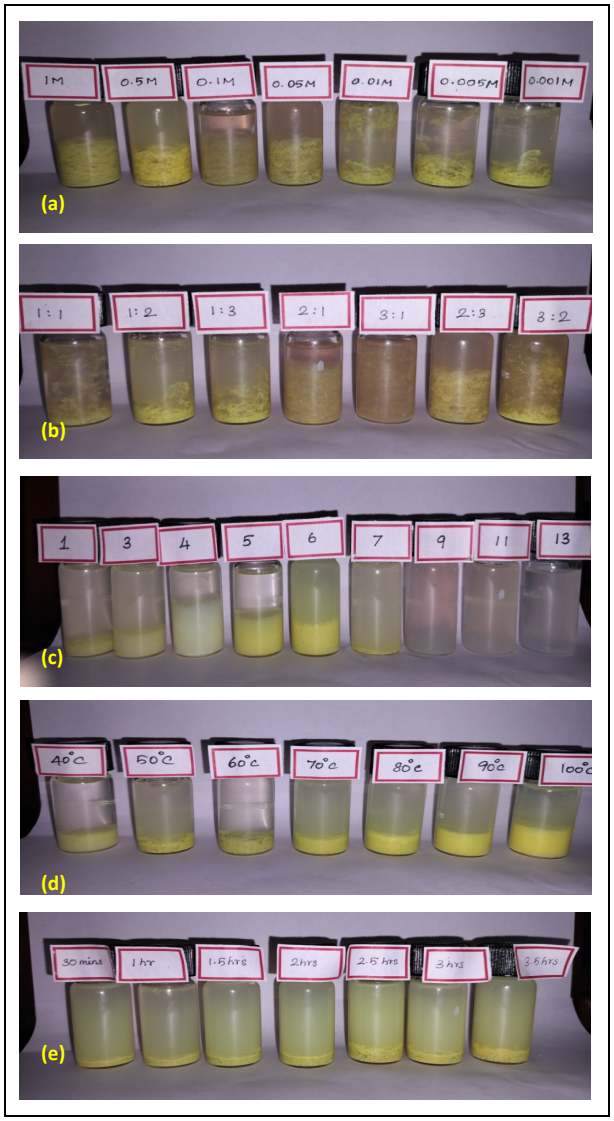

Fig. 4: Photograph showing the various optimization condition of WO_3 NPs, (a) concentration of precursor, (b) additive-precursor ratio, (c) pH condition, (d) incubation in °C and (e) reaction time

3. RESULTS AND DISCUSSION

3.1 Percentage of *Selenicereus undatus* Peel Recovery

Many fruits generate substantial peel waste, including bananas, mangoes, oranges, pineapples, watermelons and pomegranates. These fruit peels are often overlooked but are packed with valuable bioactive components like antioxidants, dietary fibers, and essential oils, making them a potential resource for various applications in food, cosmetics, and pharmaceutical industries. Similarly, in *Selenicereus undatus*, despite being discarded, the peels are rich in biologically active compounds such as betacyanin, pectins, and polyphenols, which hold significant nutritional and functional value.

$$\% \text{ Recovery of peel} = \frac{\text{Weight of SU peels (g)}}{\text{Total weight of SU (g)}} \text{ x } 100$$

$$= \frac{156.51}{332.51} x\ 100$$

$$= 47.14\ \%$$

After manually separating the pulp, the peel of *Selenicereus undatus*, accounts for approximately 47% of the entire fruit. This means that nearly 1/2 of the fruit consists of peel, making it one of the fruits with the highest proportion of peel waste.

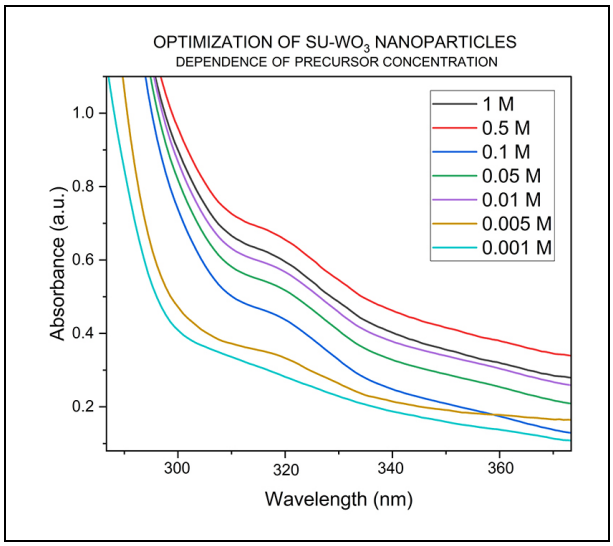

Fig. 5: Staggererd UV-Vis absorption spectrum for various precursor concentration

3.2 Optimization of WO_3 Nanoparticle Synthesis

Fig. 4 illustrates the results of visual analyses conducted to assess the formation of nanoparticles under varying experimental conditions. Changes in parameters significantly influenced the color, yield, and UV-Vis absorbance spectrum of the nanoparticles. Optimal conditions were determined by averaging the results of visual analyses and selecting the maximum absorbance wavelength (λmax) observed in the UV-Vis spectrophotometer. The concentration of sodium tungstate dihydrate ($Na_2WO_4 \cdot 2H_2O$) was systematically varied (1 M, 0.5 M, 0.1 M, 0.05 M, 0.01 M, 0.005 M, and 0.001 M), and the corresponding UV-Vis spectra are presented in Fig. 5. The results revealed that the maximum absorbance and a considerable yield were achieved at a 0.5 M concentration. Lower concentrations resulted in poor yield and significantly reduced absorbance values, indicating inadequate nanoparticle synthesis (Wantoro *et al.* 2024). Additionally, shifts in

surface plasmon resonance (SPR) peaks at these lower concentrations further underscored their unsuitability for nanoparticle production. To optimize the synthesis process, the concentration of *Selenicereus undatus* peel extract was varied in different ratios with 0.5 M $Na_2WO_4 \bullet 2H_2O$. The UV-Vis spectra for these trials are displayed in Fig. 6. The peel extract serves as a capping and stabilizing agent, preventing nanoparticle agglomeration, reducing particle size, and improving stability (Vishnupriya *et al.* 2022, Thabassoom *et al.* 2022). However, an excess amount of the extract can adversely affect the nature and purity of the nanoparticles. Based on yield, color, and UV-Vis absorbance, the ratios 2:1, 2:3, 3:2, and 1:3 were identified as favorable. Among these, the 2:1 ratio exhibited the highest λmax, followed by 2:3. Considering yield and absorbance, the 2:1 ratio was selected as the optimal condition. The pH of the reaction medium played a critical role in determining the suitability of the synthesis process (Magdy *et al.* 2023). UV-Vis spectra obtained at varying pH levels (neutral pH 7, basic pH 9, 11, 13, and acidic pH 1, 3, 4, 5) are shown in Fig. 7. Basic conditions resulted in lower absorbance values, indicating that they were unfavorable for nanoparticle synthesis (Hemmatzadeh *et al.* 2024). Similarly, higher acidic pH levels (pH 1, 3, and 4) produced lower yields and improper color development, suggesting incomplete or defective nanoparticle formation. Among the tested conditions, pH 5 emerged as the most suitable, as it provided the best combination of yield and λmax. Incubation temperature is a critical factor in determining nanoparticle yield and quality (Fatiha *et al.* 2022). The UV-Vis spectra for different incubation temperatures (40°C, 50°C, 60°C, 70°C, 80°C, 90°C, and 100°C) are depicted in Fig. 8. The results indicated that higher temperatures improved the synthesis process, with the optimal temperature identified as 100°C. At this temperature, the residue exhibited maximum absorbance and a significantly higher yield. The incubation time was varied from 30 minutes to 3.5 hours to assess its impact on nanoparticle formation. The corresponding UV-Vis spectra are shown in Fig. 9. The results demonstrated a progressive increase in yield with longer incubation times. Among the tested durations, the yield was relatively high for incubation times of 2.5 hours, 3 hours, and 3.5 hours. The maximum absorbance, however, was observed at 2.5 hours, suggesting this as the optimal incubation time for achieving efficient nanoparticle synthesis (Divakaran *et al.* 2019).

3.3 Characterization of WO_3 NPs

The optical property of the synthesized WO_3 NPs was analyzed using UV-DRS spectroscopy. A sharp absorption edge was observed around 308 nm indicating the material's ability to absorb UV light effectively, and the corresponding Tauc plot indicated bandgap energy of 2.23 eV, as shown in Fig. 10 (a) and (b). This absorption is characteristic of the electronic transitions in WO_3, associated with charge transfer from the valence band (O 2p) to the conduction band (W 5d). The Tauc plot was generated using the Tauc and Davis-Mott model, where the WO_3 is an indirect bandgap semiconductor (n= ½) (Zhou *et al.* 2023).

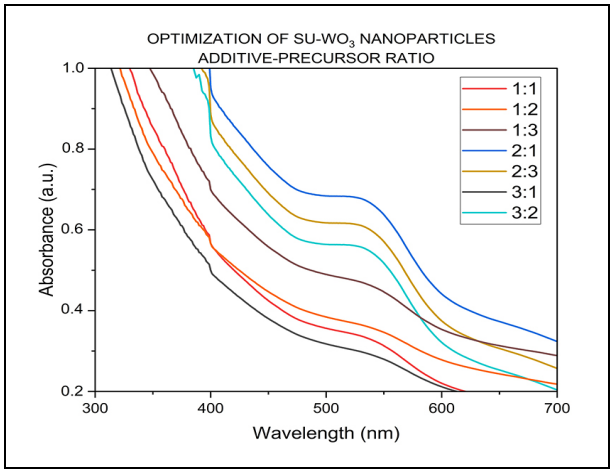

Fig. 6: Staggererd UV-Vis absorption spectrum for various additive-precursor concentration

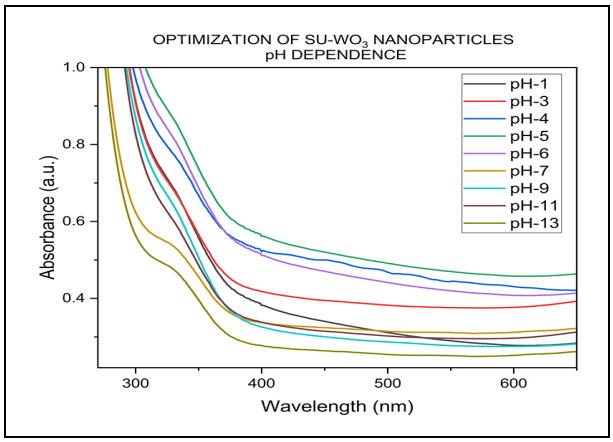

Fig. 7: Staggererd UV-Vis absorption spectrum for various pH

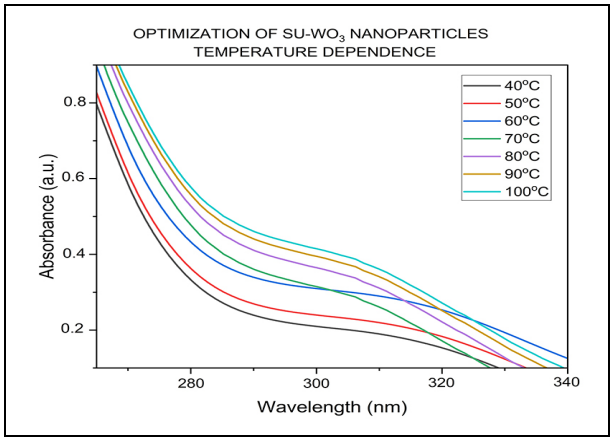

Fig. 8: Staggererd UV-Vis absorption spectrum for various temperature

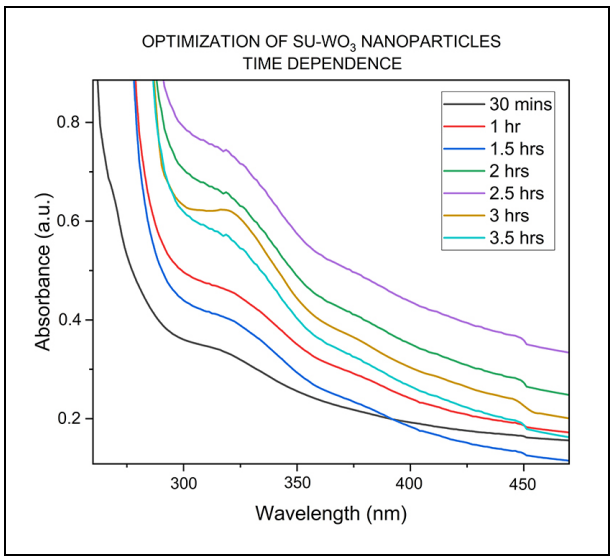

Fig. 9: Staggererd UV-Vis absorption spectrum for various reaction time

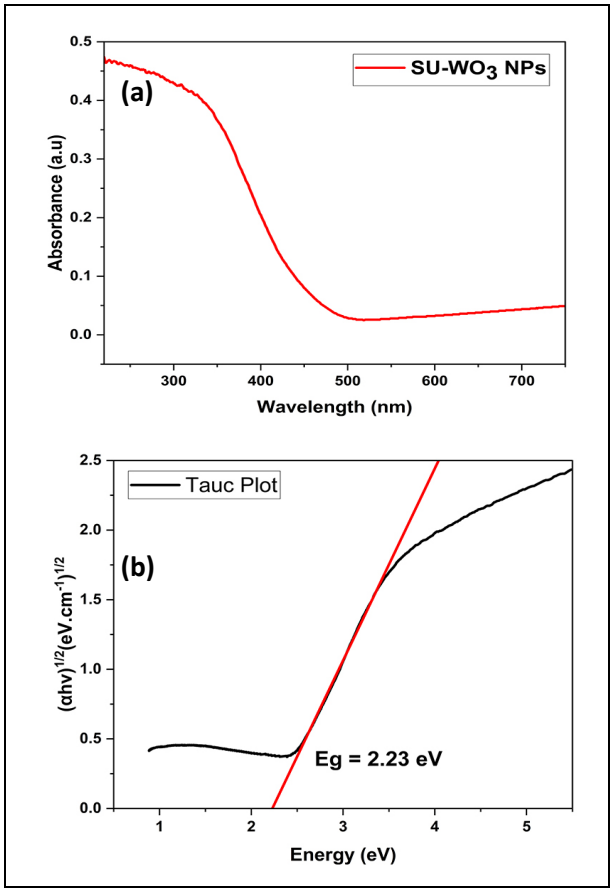

Fig. 10: (a) UV-DRS spectrum of WO_3 NPs and (b) Tauc plot

The FTIR spectrum of the synthesized WO_3 NPs is presented in Fig. 11. The key functional groups confirming the presence of WO_3 are identified by the peaks at 942.52 cm^{-1} and 680.38 cm^{-1} (Veerakumar *et al.* 2023). The strong band at 942.52 cm^{-1} corresponding to W=O stretching vibrations is indicative of terminal tungsten-oxygen double bonds, while the peak at 680.38 cm^{-1} is attributed to W-O-W bending vibrations, confirming the structural framework of WO_3 (Shaikh *et al*. 2022). Additionally, the broad band at 3399.15 cm^{-1} represents O-H stretching vibrations from adsorbed water or surface hydroxyl groups. The peak at 2925.06 cm^{-1} is associated with C-H stretching, likely from organic residues. The band at 1622.42 cm^{-1} corresponds to O-H bending, and the peaks at 1462.19 cm^{-1} and 1384.26 cm^{-1} are attributed to bending vibrations of residual organic groups (Kumar *et al*. 2017).

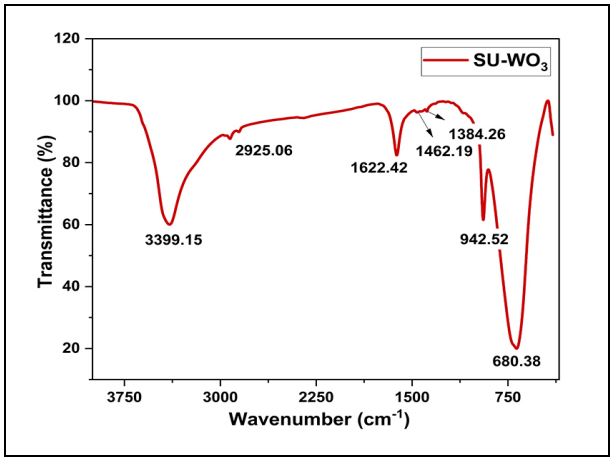

Fig. 11: FTIR spectrum of WO_3 NPs

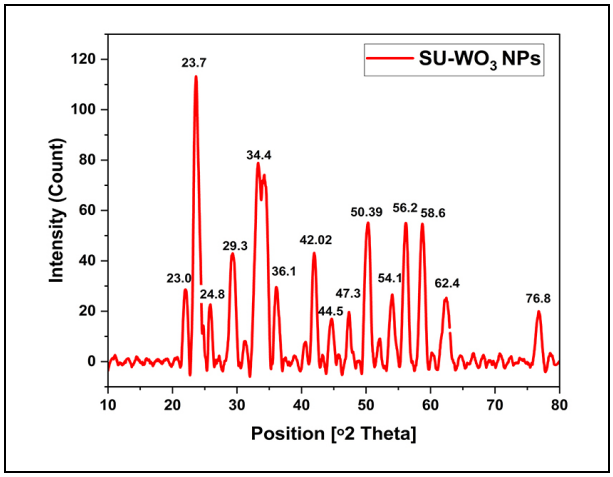

Fig. 12: XRD spectrum of WO_3 NPs

The XRD pattern of WO_3 NPs showed in Fig. 12, exhibits sharp and well-defined peaks, confirming their crystalline nature. The most intense peak at 2θ = 23.7° corresponds to the (002) plane, indicating the monoclinic phase of WO_3, as verified by the JCPDS card (43-1035). Other prominent peaks are observed at 2θ values of 23.0, 24.8, 29.3°, 34.4°, 36.1°, 42.02°, 47.3°, 50.39°, 54.1°, 56.2° and 58.6°, corresponding to planes such as (020), (200), (120), (112), (022), (202), (202), (222), (004), (140) and (420) (Dawadi *et al.* 2021). The

average crystalline size of WO_3 NPs was determined to be 41.57 nm, calculated using the Debye-Scherrer equation.

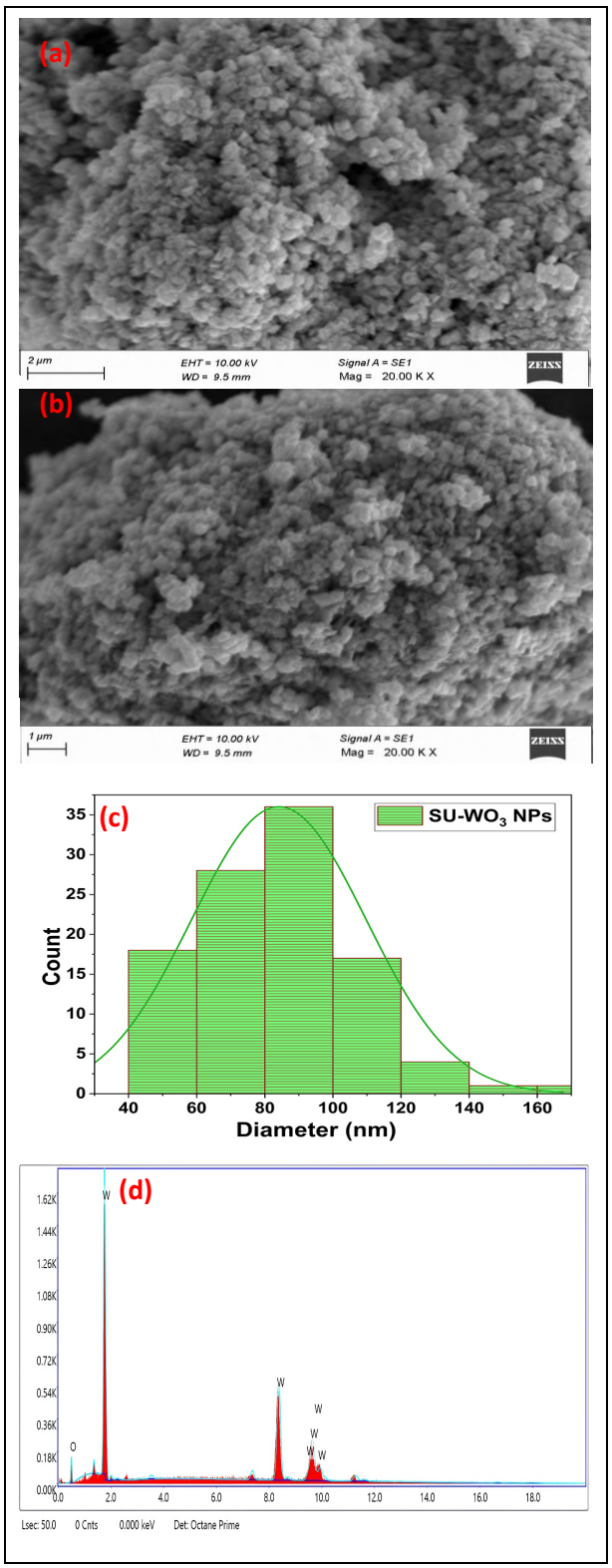

Fig. 13: (a)-(b) SEM image of WO_3 NPs, (c) Histogram of WO_3 NPs, (d) EDAX spectrum of WO_3 NPs

The SEM images, depicted in Fig. 13 (a) and (b), reveal the morphology of WO_3 NPs at high magnification (20.00 KX). The particle exhibits polyhedral-shaped WO_3 NPs with uniform morphology, confirming their nanoscale dimensions. The histogram illustrates the particle size distribution of WO_3. The histogram illustrates the particle size distribution of WO_3 NPs (Fig. 13 (c)) with a mean size of approximately 84 nm, with most particles falling between 60 and 100 nm, demonstrating consistent synthesis (Bayahia, 2022). This narrow distribution indicates consistent synthesis with minimal variation in particle size. The EDAX spectrum (Fig. 13 (d)) confirms the elemental composition of the WO_3 nanoparticles. Prominent tungsten (W) peaks dominate the spectrum, along with a minor oxygen (O) peak, confirming the presence of tungsten trioxide as the synthesized material.

The zeta potential of the synthesized WO_3 NPs displayed in Fig. 14, was measured as -24.4 mV with a standard deviation of 5.89 mV, indicating moderate colloidal stability. The zeta potential distribution showed a dominant peak at -24.5 mV, accounting for 99.5% of the total area, while minor peaks were negligible. The measured conductivity was 0.0719 mS/cm, and the result quality was deemed good. This value suggests sufficient electrostatic repulsion between particles to prevent significant agglomeration, contributing to the stability of the colloidal system in an aqueous medium (Shet *et al.* 2023, Shahinuzzaman *et al.* 2024).

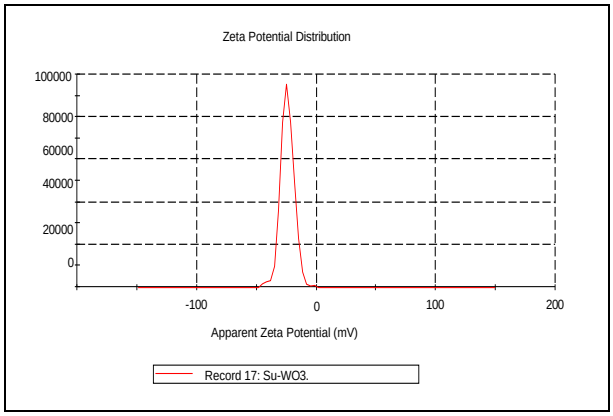

Fig. 14: Zeta potential of WO_3 NPs

DLS analysis of the synthesized WO_3 NPs, shown in Fig. 15, revealed an average hydrodynamic diameter of 83.1 nm, with a polydispersity index (P.I.) of 0.313, indicating a uniform size distribution. The intensity distribution showed a prominent peak at 105.9 nm, representing the majority of the particles, and a smaller but notable peak at 1.3 nm with a standard deviation of 0.2 nm. The overall size distribution, with an average diameter of 100 nm, confirms the effective synthesis of WO_3 NPs with diverse size ranges, making

them suitable for applications requiring multi-scale properties (Ananthi *et al.* 2023, Sharma *et al*. 2020).

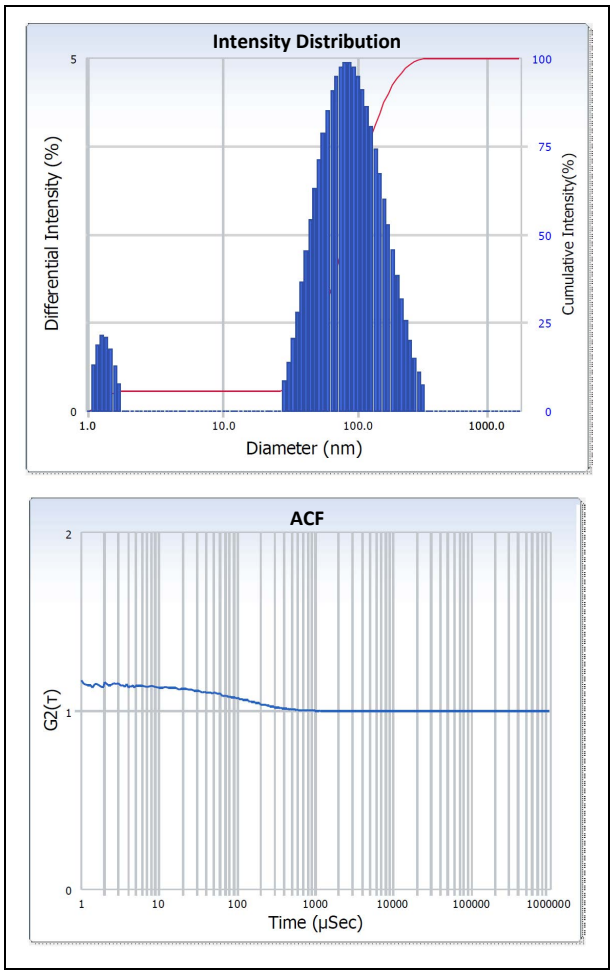

Fig. 15: DLS of WO_3 NPs

4. CONCLUSION

The current study successfully demonstrated the eco-friendly synthesis of tungsten trioxide (WO_3) nanoparticles using dragon fruit peel extract as a natural reducing and stabilizing agent under optimized conditions. UV-DRS analysis revealed a sharp absorption edge at 308 nm, with the Tauc plot indicating indirect band gap energy of 2.23 eV. FTIR confirmed the presence of W=O and W-O-W bonds, signifying the structural integrity of WO_3. The XRD analysis validated the monoclinic crystalline phase with an average crystallite size of 41.57 nm. The SEM imaging showed uniform polyhedral morphologies, while EDAX confirmed the elemental composition and purity of the nanoparticles. Zeta potential measurements of -24.4 mV highlighted good colloidal stability, and DLS analysis demonstrated an average hydrodynamic diameter of 83.1 nm, with a secondary peak at 1.3 nm, confirming a bimodal size distribution. The conductivity of 0.0719 mS/cm further validated the stability of the colloidal system. The comprehensive characterization confirms the efficacy of this green synthesis approach in producing nanoparticles with desirable physicochemical properties. This method underscores the potential of agricultural bio-waste valorization and sustainable chemistry, offering a scalable and environmentally benign alternative for advanced material synthesis. The produced WO_3 nanoparticles may exhibit promising applications in photocatalysis, environmental remediation, and sensing technologies, paving the way for future innovations in nanoscience.

FUNDING

There is no funding source.

CONFLICT OF INTEREST

The authors declared no conflict of interest in this manuscript regarding publication.

COPYRIGHT

This article is an open-access article distributed under the terms and conditions of the Creative Commons Attribution (CC BY) license (http://creativecommons.org/licenses/by/4.0/).

REFERENCES

Aminuzzaman, M., Ng, P. S., Goh, W. S., Ogawa, S. and Watanabe, A., Value-adding to dragon fruit (Hylocereus polyrhizus) peel biowaste: green synthesis of ZnO nanoparticles and their characterization, *Inorg. Nano-Metal Chem.*, 49(11), 401-411(2019). https://doi.org/10.1080/24701556.2019.1661464

Ananthi, S., Kavitha, M., Balamurugan, A., Kumar, E. R., Magesh, G., Abd El-Rehim, A. F. & Rahale, C. S., Synthesis, analysis and characterization of camellia sinensis mediated synthesis of NiO nanoparticles for ethanol gas sensor applications, *Sens. Actuators, B*, 387,133742(2023). https://doi.org/10.1016/j.snb.2023.133742

Bayahia, H., Green synthesis of activated carbon doped tungsten trioxide photocatalysts using leaf of basil (Ocimum basilicum) for photocatalytic degradation of methylene blue under sunlight, *J. Saudi Chem. Soc.*, 26(2), 101432 (2022). https://doi.org/10.1016/j.jscs.2022.101432

Dawadi, S., Katuwal, S., Gupta, A., Lamichhane, U., Thapa, R., Jaisi, S. and Parajuli, N., Current research on silver nanoparticles: synthesis, characterization, and applications, *J. Nanomater.*, *2021*(1), 6687290, (2021). https://doi.org/10.1155/2021/6687290

Divakaran, D., Lakkakula, J. R., Thakur, M., Kumawat, M. K. and Srivastava, R., Dragon fruit extract capped gold nanoparticles: Synthesis and their differential cytotoxicity effect on breast cancer cells, *Mater. Lett.*, *236*,498-502(2019). https://doi.org/10.1016/j.matlet.2018.10.156

Fatiha, L., Dwyana, Z. and Johannes, E., Silver nanoparticles synthesis from dragon fruit (Hylocereus polyrhizus) peel extract and its potential as antiseptic mouthwash, *2nd International Conference on Education and Technology*, 630, 380-386(2022). https://doi.org/10.2991/assehr.k.220103.054

Ghazal, S., Mirzaee, M. and Darroudi, M., Green synthesis of tungsten oxide (WO_3) nanosheets and investigation of their photocatalytic and cytotoxicity effects, *Micro Nano Lett.*, 17(11), 286-298(2022). https://doi.org/10.1049/mna2.12134

Hemmatzadeh, E., Bahram, M. and Dadashi, R., Photochemical modification of tea waste by tungsten oxide nanoparticle as a novel, low-cost and green photocatalyst for degradation of dye pollutant, *Spectrochim. Acta, Part A*, 313, 124104(2024). https://doi.org/10.1016/j.saa.2024.124104

Irudayaraj, A. R. S., John, F. F., Chinnasamy, D. P., Raman, K. and Joseph, A. I. J., Synthesis and characterization of Selenicereus undatus extract mediated nano-Bi_2O_3 and its application in the adsorption of Rhodamine B dye, *Zastita Materijala*, 66(1), 90-101(2025). https://doi.org/10.62638/ZasMat1188

Joice, J. A. I., Ramya, G., Florence, J. F., Kanmani, R., Rakkini, A. M., Rosaline, L. A. M. and Brindhadevi, K., Synthesis, characterization and photocatalytic activity of potassium Titanate nanocatalyst, *Appl. Nanosci.*, 13(3),2223-2232(2023). https://doi.org/10.1007/s13204-021-02117-7

Kumar, A. and Dixit, C. K., Methods for characterization of nanoparticles. Advances in nanomedicine for the delivery of therapeutic nucleic acids, *Woodhead Publishing*, 43-58 (2017). https://doi.org/10.1016/B978-0-08-100557-6.00003-1

Magdy, G., Aboelkassim, E., Abd, E. S. M. and Belal, F., A comprehensive review on silver nanoparticles: synthesis approaches, characterization techniques, and recent pharmaceutical, environmental, and antimicrobial applications, *Microchem. J.*, 196, 109615(2024). https://doi.org/10.1016/j.microc.2023.109615

Mahdi, M. A., Mohammed, M. T., Jassim, A. N. and Taay, Y. M., Green synthesis of gold NPs by using dragon fruit: Toxicity and wound healing, *Journal of Physics: Conference Series*,1853(1), 012039 (2021). https://doi.org/10.1088/1742-6596/1853/1/012039

Pechyen, C., Tangnorawich, B., Toommee, S., Marks, R. and Parcharoen, Y., Green synthesis of metal nanoparticles, characterization, and biosensing applications, *Sens. Int.*, 100287(2024). https://doi.org/10.1016/j.sintl.2024.100287

Rizvi, M., Bhatia, T. and Gupta, R.., Green & sustainable synthetic route of obtaining iron oxide nanoparticles using Hylocereus undantus (pitaya or dragon fruit), *Materials Today: Proceedings*, 50, 1100-1106(2022). http://dx.doi.org/10.1016/j.matpr.2021.07.469

Shahinuzzaman, M., Islam, M. A., Afroz, S., Hossain, M., Jamal, M. S., Alanazi, A. M. and Akhtaruzzaman, M., Synthesis of tungsten-doped zinc oxide nanoparticles using Aloe vera extracts for perovskite solar cells, *Optik*, 313, 172006(2024). https://doi.org/10.1016/j.ijleo.2024.172006

Shaikh, Y. I., Shaikh, V. S., Nazeruddin, G. M., Shekh, Z., Gugale, G. S. and Prasad, N. R., A Green Chemistry Approach towards Synthesis of Biscoumarins Catalyzed by Different Biocatalysts such as Dragon Fruit Juice, Kiwi Fruit Juice, and Buttermilk Separately by Grind Stone Technique: A Comparative Study, *ES Food & Agroforestry*, *7*(2), 25-29(2022). http://dx.doi.org/10.30919/esfaf641

Sharma, A. K. and Mathur, M., Comparative Studies on Tungsten Nanoparticles Synthesised by Chemical and Green Synthesis Route for their Toxicity Assays, *Int. J. of Pharm. Chem. Biol. Sci.*, *10*(3), 50-57(2020).

Shet, V. B., Kumar, P. S., Vinayagam, R., Selvaraj, R., Vibha, C., Rao, S. and Yumnam, S., Cocoa pod shell mediated silver nanoparticles synthesis, characterization, and their application as nanocatalyst and antifungal agent, *Appl. Nanosci.*, *13*(6), 4235-4245(2023). https://doi.org/10.1007/s13204-023-02873-8

Thabassoom, H. A. and Florence, J. F., Electroless Ni-WP Alloy Deposition on Mildsteel Using Lawsone as Complexing Agent, *Orient. J. Chem.*, *38*(6),1489(2022). http://dx.doi.org/10.13005/ojc/380622

Veerakumar, P., Hung, S. T., Hung, P. Q. and Vishnu Priya, V., Synthesis of activated porous carbon from red dragon fruit peel waste for highly active catalytic reduction in toxic organic dyes, *Catal.*, *13*(2), 449(2023). https://doi.org/10.3390/catal13020449

Vishnupriya, B., Nandhini, G. E. and Anbarasi, G., Biosynthesis of zinc oxide nanoparticles using Hylocereus undatus fruit peel extract against clinical pathogens, *Mater. Today Proc.*, *48*, 164-168 (2022). https://doi.org/10.1016/j.matpr.2020.05.474

Wantoro, A. B., Aprilia, A. and Dwandaru, W. S. B., Carbon-based nanomaterial from dragon-fruit (Hylocereus polyrhizus) peel waste as a liquid supplement for the growth of chili plant (Capsicum annuum). *IOP Conference Series: Earth and Environmental Science*, 1425(1), 012014 (2024). https://doi.org/10.52711/0974-360X.2024.00859

Zhou, X. Q., Hayat, Z., Zhang, D. D., Li, M. Y., Hu, S., Wu, Q. and Yuan, Y. Zinc oxide nanoparticles: synthesis, characterization, modification, and applications in food and agriculture, *Processes*, *11*(4), 1193(2023). https://doi.org/10.3390/pr11041193